



Published in final edited form as:

*Mol Carcinog.* 2018 November ; 57(11): 1664–1671. doi:10.1002/mc.22879.

## Low dose radiation (LDR) primed iNOS+ (M1) macrophages modulate angiogenic programming of tumor derived endothelium

Vinod Nadella<sup>1</sup>, Sandhya Singh<sup>2</sup>, Akhank Jain<sup>3</sup>, Manju Jain<sup>3</sup>, Karen M Vasquez<sup>4</sup>, Ashok Sharma<sup>5</sup>, Pranay Tanwar<sup>6</sup>, GK Rath<sup>6</sup>, Hridayesh Prakash<sup>1,6,7,8,\*</sup>

<sup>1</sup>Laboratory of Translational Medicine, School of Life Sciences, University of Hyderabad, Hyderabad, Telangana, India.

<sup>2</sup>Department of Animal Biology, School of Life Sciences, University of Hyderabad, Hyderabad, Telangana, India.

<sup>3</sup>Department of Animal Sciences, Central University of Punjab, Bathinda, Punjab, India.

<sup>4</sup>Division of Pharmacology and Toxicology, College of Pharmacy, The University of Texas at Austin, Dell Pediatric Research Institute, Austin, Texas.

<sup>5</sup>Department of Biochemistry, All India Institute of Medical Sciences, New Delhi, India.

<sup>6</sup>Dr. B.R Ambedkar Institute Rotary Cancer Hospital, All India Institute of Medical Sciences, New Delhi, India.

<sup>7</sup>Amity Institute of Virology and Immunology, Amity University, New Delhi, India.

<sup>8</sup>Translational Immunology Division, National Centre for Tumor Disease, German Cancer Research Centre, Heidelberg, Germany.

### Abstract

Solid tumors are covered by stroma, which is hypoxic in nature and composed of various non-malignant components such as endothelial cells, fibroblasts and pericytes that support tumor growth. Tumor stroma represents a mechanical barrier for tumor infiltration of CD8<sup>+</sup> effector T cells in particular. In this context, our previous studies have demonstrated the therapeutic impact of Low Dose Radiation (LDR)-primed and M1 retrained (iNOS<sup>+</sup>) peritumoral macrophages that produce inducible nitric oxide, have immunological roles on tumor infiltration of effector T cells, cancer-related inflammation, and subsequent tumor immune rejection in a mouse model of pancreatic cancer. These findings suggested a possible modification of tumor endothelium by LDR primed macrophages. In line with these observations, here we demonstrate the influence of LDR in down-modulating HIF-1 in irradiated tumors in the course of polarization of irradiated tumor associated macrophages (TAM) toward an M1 phenotype. Furthermore, we demonstrate that M1 macrophages which are primed by LDR can directly influence angiogenic responses in eNOS<sup>+</sup> endothelial cells which produce nitric oxide having both vascular and physiological roles. Furthermore we demonstrate that naïve macrophages, upon differentiating to an M1 phenotype

\* Address for correspondence with Current Affiliation: Laboratory Oncology Unit, Dr. B.R Ambedkar Institute Rotary Cancer Hospital, All India Institute of Medical Sciences (AIIMS), Ansari Nagar, 110029, New Delhi, hridayesh.prakash@gmail.com.

either by Th1 stimuli or LDR, potentially modify Sphingosine-1-Phosphate/VEGF-induced angiogenic signaling in tumor derived endothelial cells with tumorigenic potential, thus indicating the significance of iNOS+ macrophages in modulating signaling in eNOS+ tumor derived endothelium. Our study suggests that iNOS+ macrophages can activate tumor endothelium which may contribute to cancer-directed immunotherapy in particular.

## Keywords

Gamma irradiation; M1 Macrophages; Endothelium; Angiogenesis; Immune cells infiltration; Tumor Therapy

## Introduction

Tumor hypoxia and impermeable endothelium are among a variety of factors that contribute to poor prognosis and intrinsic resistance in a variety of tumors against various interventions [1–4]. Solid tumors are often surrounded with stroma rich in eNOS protein, which is important for the maintenance of the tumor microenvironment [5], endothelium energy and intrinsic resistance of tumors to variety of tumor-directed therapies [6]. Among various tissue-specific factors that contribute to endothelium energy, tumor hypoxia and high-grade tumor metabolism are key factors and characteristics of solid tumors, which render them refractory in nature [7;8]. Tumor hypoxia is executed by Hypoxia Inducible Factor 1 (HIF-1), which promotes angiogenesis, in part, by enhancing Vascular Endothelial Growth Factor (VEGF) signaling, which interferes with tumor infiltration of CD8+ and retuning of M1 phenotypic macrophages across inert endothelium [9–11]. A large variety of tumors rely on VEGF/HIF-1 and Sphingosine-1 Phosphate (S1P) which promote tumor angiogenesis. Apart from this, these tissue-derived factors also promote polarization of tumor infiltrating naïve/inflammatory macrophages toward the M2 phenotype like Tumor Associated Macrophages (TAM) [12;13].

We have previously demonstrated the indispensable role of low dose irradiation (LDR)-programmed iNOS+ (defined as M1) peritumoral macrophages in immunotherapy against non-resectable tumors of the pancreas, skin (e.g. melanoma) [14;15] and colon (Unpublished data). This was accompanied by changes in cancer related inflammation, endothelium energy and angiogenesis, which are limiting factors for tumor infiltration of T cells. Interestingly, our macrophage depletion experiments in Rip1 Tag5 mice furthermore demonstrated that selective depletion of M1 macrophages promoted glucose metabolism [15] indicating a neuroendocrine impact of LDR primed M1 macrophages in these mice.

Here, we elaborate on these findings and further demonstrate the potential of LDR in down-modulating tumor hypoxia in tumors, which may contribute to retuning of TAM toward an M1 phenotype. Interestingly, when M1 retuned macrophages were co-cultured with VEGFR2+ pancreatic  $\beta$ -islet SVR (derivative of SVEN) tumorigenic endothelium, angiogenic signaling was inhibited in these cells, which appear to have been induced by various angiogenic factors present in the tumor microenvironment. Thus, these results reveal that TAM, once polarized toward an M1 phenotype *in situ*, have the ability to activate

tumorigenic and eNOS<sup>+</sup> endothelium to facilitate tumor infiltration of effector molecules, which may contribute to immunotherapeutic approaches to the treatment of cancer.

## Material and Methods

### Antibodies and reagents

RPMI 1640, Lipopolysaccharide (LPS), Penicillin Streptomycin solution, NaNO<sub>2</sub>, Sphingosine 1 Phosphate and anti-Actin antibody were purchased from Sigma (Taufkirchen, Germany). Sulphanilamide and N-(naphthyl) ethylene-diaminedihydrochloride were purchased from E-Merck (Darmstadt, Germany). CD11b<sup>+</sup> human and Mouse MACS Microbeads and MS Columns were purchased from MiltenyiBiotec (Auburn, CA). Recombinant mouse IFN cytokines, rabbit polyclonal anti-mouse NOS2, eNOS, and pAKT and Caveolin-1 antibodies were purchased from Cell Signaling (Frankfurt, Germany). VEGFR2 and anti-HIF-1 antibodies were purchased from Novus Biological (Wiesbaden, Germany). VEGF peptide was purchased from Pepro-Tech GmbH (Hamburg, Germany). Goat anti-rabbit and mouse-HRP conjugated secondary antibodies were purchased from Sigma (Taufkirchen, Germany) and Santa Cruz (Heidelberg Germany), respectively. Mouse HIF-1 specific siRNA was purchased from Invitrogen (Schwerte, Germany). Control siRNA was purchased from Qiagen (Hilden, Germany). Goat anti-rabbit Alexa flour 488, goat anti-rat -Alexa flour 569, anti-rat-Cy3 and goat anti-mouse-Cy3 conjugated antibodies were purchased from Di-nova (Koenigswinter, Germany).

### Total body irradiation

The well characterized RipTag-5 (RT5) transgenic mouse model of spontaneous insulinoma [16] was used for this study. At ~25 weeks of age, RT5 mice were irradiated systemically with 2 Gy irradiation at weeks 25 and 26 by using a Gammatron Cobalt 60 units (Siemens, München, Germany) at a dose rate of 0.4 Gy/min. Mice were housed under pathogen-free conditions at the German Cancer Research Center. All animal experiments were authorized by the local government.

### Cell culture experiments

The RAW264.7A murine macrophage line (ATCC-TIB-71™) and the VEGFR2<sup>+</sup> mouse pancreatic  $\beta$  endothelium [17;18], also known as SVR-1 (CRL-2280) were purchased from the American Type Culture Collection (ATCC; Manassas, VA). HUVEC cells were received from Helmut Augustin, Heidelberg, Germany. These cells were co-cultured both directly and/or indirectly using a cell culture insert (Millipore, Darmstadt). For direct co-culture experiments, RAW 264.7A murine macrophage cells were seeded one day in advance of experimental use to ensure adherence. The next day, cells were washed once with serum-free media and SVR-1 cells were seeded over the monolayer of RAW macrophages and cultured for an additional 12 hours for the adherence of the tumor cells over macrophages. These cells were then treated with different stimuli for the time intervals as mentioned in the figures. For indirect cell culture, cells were cultured using a cell culture insert whereby RAW cells were cultured over the membrane and SVR cells were laid down at bottom. The RAW macrophages in the upper chamber or RAW and SVR-1 direct co-cultures were treated with various innate stimuli or irradiated by using a Gammatron Cobalt 60 unit (Siemens,

München, Germany) at a dose rate of 0.4 Gy/min. For evaluating the activation potential of irradiation and/or various stimulations, nitric oxide production was quantified in the culture supernatant by using a standard Griess reagent method [19]. For studies with CD11b+ peritoneal macrophages, C57BL/6j mice were injected with 1 mL of 4% brewer thioglycolate medium intraperitoneally and peritoneal lavage was harvested on the third day post-injection. Peritoneal lavage was centrifuged at 1500rpm for 8 min and the cell pellets were resuspended in fresh serum-free RPMI. CD11b+ macrophages were purified by using a MACS-based separation method (Miltany Biotech) and were cultured in serum-containing medium overnight. Macrophage monolayers were washed on the following day once with serum-free medium to remove any unbound cells. Cells were irradiated with different doses using a Gammatron Cobalt 60 unit (Siemens, München, Germany) at a dose rate of 0.4 Gy/min. Cells were cultured further for 48 h and the supernatants were collected and centrifuged at 5000 rpm to remove cellular debris. Next, cell-free conditioned media were collected and used for experiments as mentioned in the results.

### RNA interference

HIF-1 in RAW macrophages was depleted by using a siRNA-based method.  $1 \times 10^4$  RAW macrophages were cultured in antibiotic-free medium for 24h and were subsequently transfected with HIF-1 siRNA(SantacruzGmbH, Heidelberg, Germany) or scrambled siRNA(Invitrogen) in antibiotic- and serum-free medium with varying concentrations using an oligofactamine transfection reagent from Invitrogen (Darmstadt, Germany). The cells were incubated with the siRNA mixture for 6h in serum-free medium. The medium thereafter was replaced and cells were incubated for 24 and 48h time periods with efficiency of knockdown assessed by western analysis.

### Western analysis

Cells were washed with ice-cold PBS (pH 7.4) and lysed with RIPA buffer (50 mMTris-HCl, pH 7.4, 150 mMNaCl, 2 mMEDTA, 1% Nonidet P-40, and a protease inhibitor mixture) and sonicated. The lysate was centrifuged at 14,000 rpm for 20 min at 4°C to separate the particulate fraction. Protein concentration was determined by using a BCA kit (Darmstadt, Germany). 20µg protein per sample was separated on a Nu-PAGE Bis-Tris Mini Gel system and blotted onto a PVDF membrane. Blots were blocked at room temperature for 30 minutes with 5% nonfat dry milk in TBS-T (20 mMTris base, 137 mMNaCl, and 0.05% Tween 20, pH 7.5) and then incubated overnight at 4°C with primary antibodies, and subsequently incubated with horseradish peroxidase-conjugated secondary antibodies. Blots were visualized by using an ECL reagent (GE Healthcare, Dornstadt, Germany) β-actin was used an internal loading control.

### Fluorimetric analysis

Various intracellular signaling proteins were measured by using a Fluorimetric method [14;20]. Briefly, cells were cultured in flat bottom black 96 well plates and subsequently irradiated, stimulated and incubated for various time intervals, as mentioned. After incubation, the cell monolayers were washed once with PBS and fixed with 4% PFA for 10–15 minutes at room temperature and permeabilized with 0.1% Triton X for 5 minutes. The cell layers were then blocked in PBS containing 1% BSA and 1% serum from the host of

secondary antibodies. Next, the cell layers were incubated with primary antibody at 4°C overnight in the dark. The next day, the cells were washed twice with 1X PBS. The cells were then incubated with Alexa Fluor-conjugated secondary antibodies (Invitrogen) for 1h at room temperature in the dark. The cell layers were washed again twice with PBS. The plates were read at 488nm for Alexa-Fluor488 labeled antibodies or at 594nm for Alexa-Fluor 594 labeled antibodies respectively, with a reference wavelength of 630 nm using a 96 well fluorimeter (TECAN Infinite 200 PRO Systems, Mainz, Germany). Each sample/well was read at multiple fields for uniformity and the mean fluorescence intensities of stained cells from each well were calculated.

### Statistical analysis

All results were expressed as the mean  $\pm$  SEM of 3 independent experiments performed in triplicates. Statistical analyses were conducted using either Student's t tests, 1 way or 2 way ANOVA followed by Bonferroni post-test (\*P < 0.05; \*\*P < 0.01; \*\*\*P < 0.001). All the statistical analyses were carried analyzed using GraphPad Prism Version 7.0 software.

## Results and Discussion

### Dual role of HIF-1 in macrophage polarization

Whole body Irradiation of insulinoma bearing RipTag5 mice led to the complete degradation of HIF-1 in the tumors of treated mice (Fig. 1A), which correlated with the reduced levels of key angiogenic proteins in these tumors and M1 retuning of TAM in these mice [14;15]. Degradation of HIF-1 and concurrent upregulation of iNOS in the irradiated tumors and purified CD11b+ TAM from insulinoma-bearing mice [14;15] indicated that depletion of HIF-1 following irradiation may contribute in the upregulation of iNOS in macrophages in these mice [14]. On the basis of these results, we anticipated that HIF-1 depletion would enhance NO levels in macrophages. To test this, we depleted HIF-1 in RAW macrophages using an siRNA-based approach and NO levels were measured in the culture supernatants. Consistent with our hypothesis, depletion of HIF-1 in these macrophages enhanced NO levels, particularly in the irradiated macrophages (Fig 1B), which is in line with recent reports [21;22] and our published data [14].

HIF-1 is a master transcription factor and when stabilized, in addition to executing hypoxia related physiological responses, it also promotes angiogenic signaling in the polarization of tumor infiltrating Th1 primed macrophages [23;24]. To test this, we stabilized HIF-1 in the naïve macrophages by treating them with a hypoxia-mimetic agent, CoCl<sub>2</sub> [25;26] and treated the cells with Th1 stimuli. Indeed, the results from these experiments suggested that stabilization of HIF-1 in the macrophages significantly inhibited the generation of NO in the culture supernatant of iNOS+ Th1-primed inflammatory macrophages (Fig. 1C). These findings correlated with results in M1 programming of irradiated TAM in RipTag5 mice. Several studies with HIF-1 specific knockout animals have demonstrated the contribution of HIF-1 proteins in Th1 effector responses of iNOS+ and infected macrophages [22;27;28]. Thus, HIF-1 expression is likely an important contributor to M1 programming of naïve macrophages in tumor-free environments, suggesting a dual fate of HIF-1 on macrophage polarization. To clarify this, naïve RAW macrophages were treated with different

concentrations of CoCl<sub>2</sub> and NO titers in treated cell culture supernatants were quantified. Supporting our hypothesis, the results indicated that low levels of HIF-1 enhanced NO titers in naïve RAW macrophages (Fig 1D), suggesting that low levels of HIF-1 support the differentiation of naïve macrophages toward an M1 phenotype. Surprisingly, an increase in the expression levels of iNOS proteins after treatment with CoCl<sub>2</sub> in purified CD11b<sup>+</sup> macrophages from Rip Tag5 mice demonstrated the influence of HIF-1 stabilization on re-polarization of TAMs in this system (Fig. 1E). Tissue/tumor hypoxia is known to control both macrophage activation as well their tissue infiltration during inflammatory responses. For example, a recent report suggested that HIF-1 promotes the expression of CD68 and CCL2 and enhanced macrophage recruitment in tumor tissues [29–31]. Whether HIF-1 promotes M1 or M2 phenotypes in macrophages may depend upon the increased expression of HIF-2 proteins for which the presence of active HIF-1 is essential. Stabilization of HIF-2 in macrophages promoted the degradation of HIF-1 in a protease-dependent manner and in such chronic conditions, HIF-2 could promote M2 polarization in macrophages. Interestingly, low dose irradiation of macrophages led to the activation of HIF-1 in naïve HIF-2 negative macrophages [14]. These results reinforced that the notion that the presence of HIF-2 and associated signaling pathways, including non-canonical nf-KB and TGF- $\beta$  in macrophages [32;33] are important for dictating the fate of HIF-1 for macrophage activation. Thus, these results provide a potential explanation for the dual fate of HIF on NO levels [34;35] and its balance in inflamed macrophages, which may be useful for tumor therapy and open new lines of investigation.

### **Tumor derived endothelium inhibits Th1 programming of naïve macrophages**

To determine whether tumorigenic endothelium would influence iNOS<sup>+</sup> macrophages or not, we co-cultured VEGFR2<sup>+</sup> SVR-1 with RAW macrophages directly or indirectly and measured NO levels (both constitutive and inducible) in the cultured supernatant. The influence of RAW macrophages was analyzed on the expression of various angiogenic proteins in RAW co-cultured SVR-1 cells. We found that co-cultures of SVR-1 cells and naïve macrophages enhanced the constitutive NO levels in culture supernatants, but this remained insignificant over RAW macrophages alone (Fig. 2A). However, SVR-1 inhibited the levels of inducible NO in the culture supernatant of Th1 primed iNOS<sup>+</sup> macrophages (Fig. 2B), suggesting that SVR-1 assisted in driving the polarization of these macrophages to either M2 or TAM phenotypes. This may be due to VEGF-R2-mediated angiogenic programming of RAW macrophages [36;37], which was evident with the drop of inducible NO in the co-cultures (Fig. 2B) treated with key angiogenic factors in tumors such as S1P and VEGF.

### **LDR-primed M1 macrophages modulate tumor-derived endothelium**

Our previous studies have demonstrated the influence of low dose radiation on the activation of tumor endothelium for permitting the tumor infiltration of immune effector cells in the rejection of established tumors. This provoked us to analyze whether gamma irradiation would influence angiogenic signaling in tumor endothelium directly or not. To test this, we irradiated both tumor derived endothelial cells (SVR-1 cells) and primary HUVEC with 2 Gy of irradiation and analyzed the expression of various angiogenic proteins in tumor-derived endothelial cells. We found that irradiation of these tumorigenic SVR-1 cells



inhibited the levels of eNOS in both SVR-1 (Fig 3A–B) and HUVEC cells (Fig 4), confirming reduced levels of eNOS in irradiated insulinoma [14]. This could be due to reduced levels of HSP90 protein, a major chaperone of eNOS proteins in the activated endothelium in irradiated tumors [14;15]. Interestingly, Low Dose Radiation enhanced the expression of Caveolin-1 proteins in SVR-1 cells, in line with our previous findings [14;15]. However, radiation did not modify the expression of pAKT significantly in these endothelial cells. These results suggested that Low Dose Radiation has the potential of mitigating eNOS signaling, which is largely influenced by VEGF and other tumor-derived angiogenic factors in endothelium that likely contributes to their increased permeability to endothelium in stromal tissues.

We have previously demonstrated that the LDR-driven iNOS<sup>+</sup> M1 phenotype [14] is decisive for tumor vasculature normalization, enhanced tumor infiltration of T cells, and subsequent tumor immune rejection in RipTag5 mice [14, 15]. On the basis of these results, we anticipated that iNOS<sup>+</sup> macrophages would influence angiogenic signaling in tumorigenic endothelium. To test this presumption, we cultured SVR-1 cells in the presence of conditioned media from irradiated CD11b<sup>+</sup> mouse primary macrophages that had acquired an M1 phenotype post irradiation [14], and analyzed the expression of eNOS proteins. Following our expectation, conditioned media from 2Gy irradiated primary macrophages by their virtue of the M1 phenotype [14], inhibited the expression of eNOS in SVR-1 (Fig. 3C–D) and HUVEC cells (Fig 4A–D). These results further confirmed the angiostatic impact of LDR-primed iNOS<sup>+</sup> macrophages. Further, low dose gamma irradiation directly or via LDR-primed macrophages reduced the levels of S1P and VEGF induced angiogenic proteins in HUVEC cells. This is likely due to the presence of various Th1 effector cytokines (e.g. IFN- $\gamma$  and TNF- $\alpha$ ) in the conditioned media of 2Gy-exposed macrophages [14]. Thus, these data not only corroborated our previous studies [15] where depletion of iNOS proteins in insulinoma bearing RipTag5 mice enhanced tumor-related inflammation, T cell infiltration [15], and inhibited pro-inflammatory responses, but also reinforced the involvement of iNOS proteins in modulating the angiogenic responses in tumors, which is one of the key hurdles in cancer therapy.

## Acknowledgements

This work was supported by a Ramanujan grant from the Department of Science and Technology (SR/S2/RJN/03/2012) to HP.

Funding information

Science and Engineering Research Board. Grant Number SR/S2/RJN/03/2012

National Institute of Health/ National Cancer Institute (NIH/NCI). Grant Number: CA093279

## Reference List

1. Jain RK, Duda DG, Willett CG, Sahani DV, Zhu AX, Loeffler JS, Batchelor TT, and Sorensen AG (2009) Biomarkers of response and resistance to antiangiogenic therapy. *Nat.Rev.Clin.Oncol*, 6, 327–338. [PubMed: 19483739]
2. Jain RK (2009) A new target for tumor therapy. *N.Engl.J.Med*, 360, 2669–2671. [PubMed: 19535806]

3. Jain RK (2014) Antiangiogenesis strategies revisited: from starving tumors to alleviating hypoxia. *Cancer Cell*, 26, 605–622. [PubMed: 25517747]
4. Kheshtchin N, Arab S, Ajami M, Mirzaei R, Ashourpour M, Mousavi N, Khosravianfar N, Jadidi-Niaragh F, Namdar A, Noorbakhsh F, and Hadjati J (2016) Inhibition of HIF-1 $\alpha$  enhances anti-tumor effects of dendritic cell-based vaccination in a mouse model of breast cancer. *Cancer Immunol.Immunother*, 65, 1159–1167. [PubMed: 27497816]
5. Lim KH, Ancrile BB, Kashatus DF, and Counter CM (2008) Tumour maintenance is mediated by eNOS. *Nature*, 452, 646–649. [PubMed: 18344980]
6. Bouzin C, Brouet A, De VJ, Dewever J, and Feron O (2007) Effects of vascular endothelial growth factor on the lymphocyte-endothelium interactions: identification of caveolin-1 and nitric oxide as control points of endothelial cell anergy. *J.Immunol*, 178, 1505–1511. [PubMed: 17237399]
7. Liu J, Zhang J, Wang X, Li Y, Chen Y, Li K, Zhang J, Yao L, and Guo G (2010) HIF-1 and NDRG2 contribute to hypoxia-induced radioresistance of cervical cancer Hela cells. *Exp.Cell Res*, 316, 1985–1993. [PubMed: 20206160]
8. Hong SS, Lee H, and Kim KW (2004) HIF-1 $\alpha$ : a valid therapeutic target for tumor therapy. *Cancer Res.Treat*, 36, 343–353. [PubMed: 20368827]
9. Lapeyre-Prost A, Terme M, Pernot S, Pointet AL, Voron T, Tartour E, and Taieb J (2017) Immunomodulatory Activity of VEGF in Cancer. *Int.Rev.Cell Mol.Biol*, 330, 295–342. [PubMed: 28215534]
10. Thomas AA, Fisher JL, Hampton TH, Christensen BC, Tsongalis GJ, Rahme GJ, Whipple CA, Steel SE, Davis MC, Gaur AB, Lewis LD, Ernstoff MS, and Fadul CE (2017) Immune modulation associated with vascular endothelial growth factor (VEGF) blockade in patients with glioblastoma. *Cancer Immunol.Immunother*, 66, 379–389. [PubMed: 27942839]
11. Voron T, Marcheteau E, Pernot S, Colussi O, Tartour E, Taieb J, and Terme M (2014) Control of the immune response by pro-angiogenic factors. *Front Oncol*, 4, 70. [PubMed: 24765614]
12. Yoshida GJ (2015) Metabolic reprogramming: the emerging concept and associated therapeutic strategies. *J.Exp.Clin.Cancer Res*, 34, 111. [PubMed: 26445347]
13. Cairns RA, Papandreou I, Sutphin PD, and Denko NC (2007) Metabolic targeting of hypoxia and HIF1 in solid tumors can enhance cytotoxic chemotherapy. *Proc.Natl.Acad.Sci.U.S.A*, 104, 9445–9450. [PubMed: 17517659]
14. Prakash H, Klug F, Nadella V, Mazumdar V, Schmitz-Winnenthal H, and Umansky L (2016) Low doses of gamma irradiation potentially modifies immunosuppressive tumor microenvironment by retuning tumor-associated macrophages: lesson from insulinoma. *Carcinogenesis*, 37, 301–313. [PubMed: 26785731]
15. Klug F, Prakash H, Huber PE, Seibel T, Bender N, Halama N, Pfirschke C, Voss RH, Timke C, Umansky L, Klapproth K, Schakel K, Garbi N, Jager D, Weitz J, Schmitz-Winnenthal H, Hammerling GJ, and Beckhove P (2013) Low-dose irradiation programs macrophage differentiation to an iNOS(+)/M1 phenotype that orchestrates effective T cell immunotherapy. *Cancer Cell*, 24, 589–602. [PubMed: 24209604]
16. Hanahan D (1985) Heritable formation of pancreatic beta-cell tumours in transgenic mice expressing recombinant insulin/simian virus 40 oncogenes. *Nature*, 315, 115–122. [PubMed: 2986015]
17. Shevchenko I, Karakhanova S, Soltak S, Link J, Bayry J, Werner J, Umansky V, and Bazhin AV (2013) Low-dose gemcitabine depletes regulatory T cells and improves survival in the orthotopic Panc02 model of pancreatic cancer. *Int.J.Cancer*, 133, 98–107. [PubMed: 23233419]
18. Guleng B, Tateishi K, Ohta M, Kanai F, Jazag A, Ijichi H, Tanaka Y, Washida M, Morikane K, Fukushima Y, Yamori T, Tsuruo T, Kawabe T, Miyagishi M, Taira K, Sata M, and Omata M (2005) Blockade of the stromal cell-derived factor-1/CXCR4 axis attenuates in vivo tumor growth by inhibiting angiogenesis in a vascular endothelial growth factor-independent manner. *Cancer Res*, 65, 5864–5871.
19. Giustarini D, Rossi R, Milzani A, and Dalle-Donne I (2008) Nitrite and nitrate measurement by Griess reagent in human plasma: evaluation of interferences and standardization. *Methods Enzymol*, 440, 361–380. [PubMed: 18423230]



20. Prakash H, Nadella V, Singh S, and Schmitz-Winnenthal H (2016) CD14/TLR4 priming potentially recalibrates and exerts anti-tumor efficacy in tumor associated macrophages in a mouse model of pancreatic carcinoma. *Sci.Rep*, 6, 31490. [PubMed: 27511884]
21. Matak P, Heinis M, Mathieu JR, Corriden R, Cuvellier S, Delga S, Mounier R, Rouquette A, Raymond J, Lamarque D, Emile JF, Nizet V, Touati E, and Peyssonnaud C (2015) Myeloid HIF-1 is protective in Helicobacter pylori-mediated gastritis. *J.Immunol*, 194, 3259–3266. [PubMed: 25710915]
22. Bhandari T and Nizet V (2014) Hypoxia-Inducible Factor (HIF) as a Pharmacological Target for Prevention and Treatment of Infectious Diseases. *Infect.Dis.Ther*, 3, 159–174. [PubMed: 25134687]
23. Werno C, Menrad H, Weigert A, Dehne N, Goerdts S, Schledzewski K, Kzhyshkowska J, and Brune B (2010) Knockout of HIF-1 $\alpha$  in tumor-associated macrophages enhances M2 polarization and attenuates their pro-angiogenic responses. *Carcinogenesis*, 31, 1863–1872. [PubMed: 20427344]
24. Doedens AL, Stockmann C, Rubinstein MP, Liao D, Zhang N, DeNardo DG, Coussens LM, Karin M, Goldrath AW, and Johnson RS (2010) Macrophage expression of hypoxia-inducible factor-1  $\alpha$  suppresses T-cell function and promotes tumor progression. *Cancer Res*, 70, 7465–7475. [PubMed: 20841473]
25. Piret JP, Mottet D, Raes M, and Michiels C (2002) CoCl<sub>2</sub>, a chemical inducer of hypoxia-inducible factor-1, and hypoxia reduce apoptotic cell death in hepatoma cell line HepG2. *Ann.N.Y.Acad.Sci*, 973, 443–447. [PubMed: 12485908]
26. Ardyanto TD, Osaki M, Tokuyasu N, Nagahama Y, and Ito H (2006) CoCl<sub>2</sub>-induced HIF-1 $\alpha$  expression correlates with proliferation and apoptosis in MKN-1 cells: a possible role for the PI3K/Akt pathway. *Int.J.Oncol*, 29, 549–555. [PubMed: 16865270]
27. Matak P, Heinis M, Mathieu JR, Corriden R, Cuvellier S, Delga S, Mounier R, Rouquette A, Raymond J, Lamarque D, Emile JF, Nizet V, Touati E, and Peyssonnaud C (2015) Myeloid HIF-1 is protective in Helicobacter pylori-mediated gastritis. *J.Immunol*, 194, 3259–3266. [PubMed: 25710915]
28. Kempf VA, Lebedziejewski M, Alitalo K, Walzlein JH, Eehalt U, Fiebig J, Huber S, Schutt B, Sander CA, Muller S, Grassl G, Yazdi AS, Brehm B, and Autenrieth IB (2005) Activation of hypoxia-inducible factor-1 in bacillary angiomatosis: evidence for a role of hypoxia-inducible factor-1 in bacterial infections. *Circulation*, 111, 1054–1062. [PubMed: 15723970]
29. Guo X, Xue H, Shao Q, Wang J, Guo X, Chen X, Zhang J, Xu S, Li T, Zhang P, Gao X, Qiu W, Liu Q, and Li G (2016) Hypoxia promotes glioma-associated macrophage infiltration via periostin and subsequent M2 polarization by upregulating TGF- $\beta$  and M-CSFR. *Oncotarget*, 7, 80521–80542. [PubMed: 27602954]
30. Chai CY, Chen WT, Hung WC, Kang WY, Huang YC, Su YC, and Yang CH (2008) Hypoxia-inducible factor-1 $\alpha$  expression correlates with focal macrophage infiltration, angiogenesis and unfavourable prognosis in urothelial carcinoma. *J.Clin.Pathol*, 61, 658–664. [PubMed: 17908805]
31. Li N, Li Y, Li Z, Huang C, Yang Y, Lang M, Cao J, Jiang W, Xu Y, Dong J, and Ren H (2016) Hypoxia Inducible Factor 1 (HIF-1) Recruits Macrophage to Activate Pancreatic Stellate Cells in Pancreatic Ductal Adenocarcinoma. *Int.J.Mol.Sci*, 17.
32. Joshi S, Singh AR, Zulcic M, and Durden DL (2014) A macrophage-dominant PI3K isoform controls hypoxia-induced HIF1 $\alpha$  and HIF2 $\alpha$  stability and tumor growth, angiogenesis, and metastasis. *Mol.Cancer Res*, 12, 1520–1531. [PubMed: 25103499]
33. Sluimer JC, Gasc JM, van Wanroij JL, Kisters N, Groeneweg M, Sollewijn Gelpke MD, Cleutjens JP, van den Akker LH, Corvol P, Wouters BG, Daemen MJ, and Bijnens AP (2008) Hypoxia, hypoxia-inducible transcription factor, and macrophages in human atherosclerotic plaques are correlated with intraplaque angiogenesis. *J.Am.Coll.Cardiol*, 51, 1258–1265. [PubMed: 18371555]
34. Dehne N and Brune B (2009) HIF-1 in the inflammatory microenvironment. *Exp.Cell Res*, 315, 1791–1797. [PubMed: 19332053]
35. Takeda N, O’Dea EL, Doedens A, Kim JW, Weidemann A, Stockmann C, Asagiri M, Simon MC, Hoffmann A, and Johnson RS (2010) Differential activation and antagonistic function of HIF-1 $\alpha$  isoforms in macrophages are essential for NO homeostasis. *Genes Dev*, 24, 491–501. [PubMed: 20194441]

36. Yang KS, Lim JH, Kim TW, Kim MY, Kim Y, Chung S, Shin SJ, Choi BS, Kim HW, Kim YS, Chang YS, Kim HW, and Park CW (2014) Vascular endothelial growth factor-receptor 1 inhibition aggravates diabetic nephropathy through eNOS signaling pathway in db/db mice. *PLoS.One*, 9, e94540. [PubMed: 24759928]
37. Jin ZG, Ueba H, Tanimoto T, Lungu AO, Frame MD, and Berk BC (2003) Ligand-independent activation of vascular endothelial growth factor receptor 2 by fluid shear stress regulates activation of endothelial nitric oxide synthase. *Circ.Res*, 93, 354–363. [PubMed: 12893742]

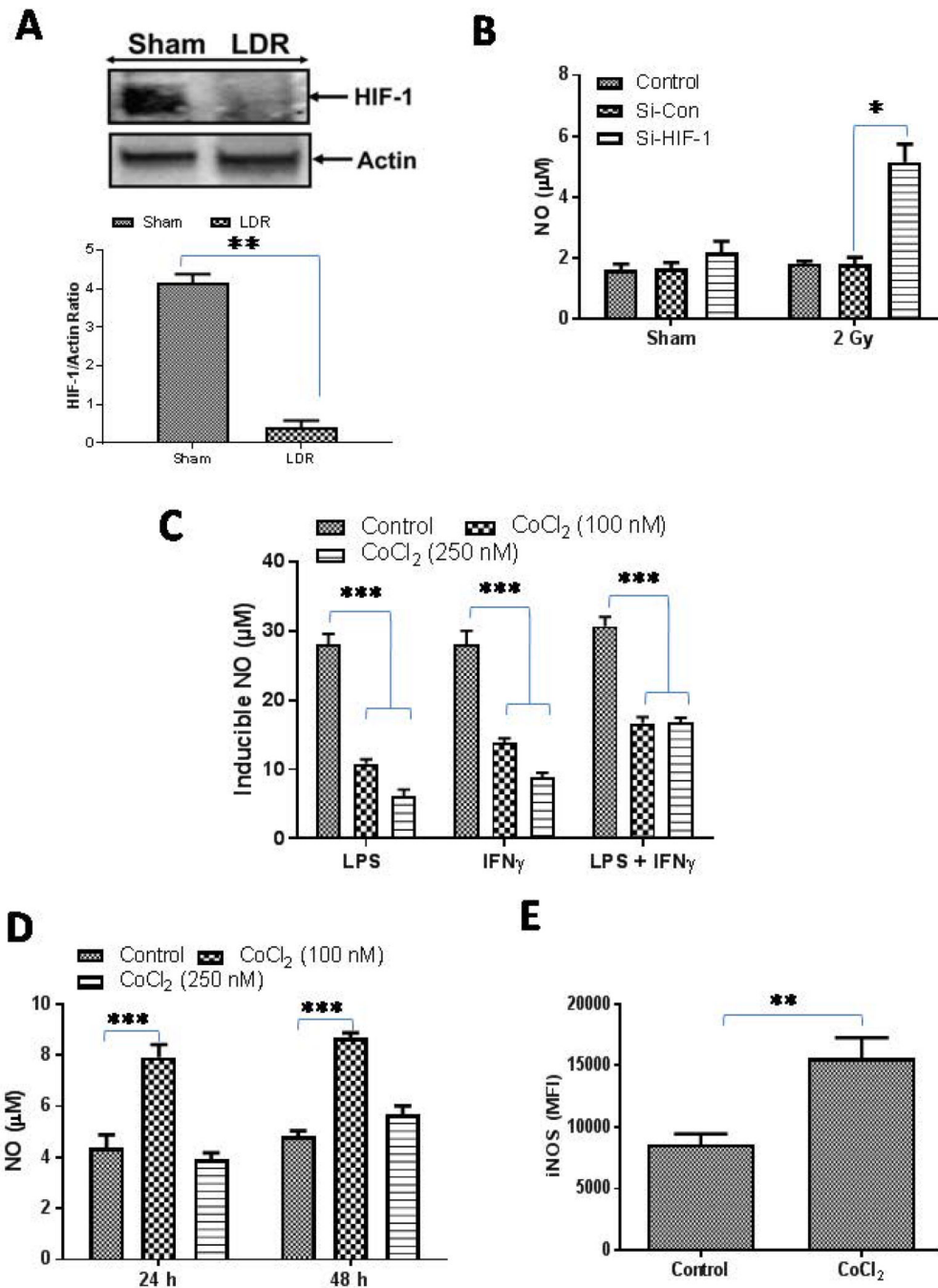
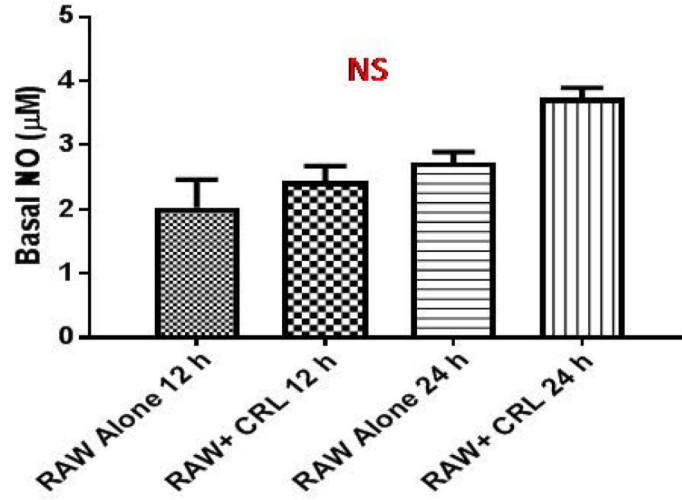


**Figure 1. Dual role of HIF-1 in macrophage retuning.**

**(A)** RT5 mice (25 weeks of age) were treated twice with 2 Gy irradiation and were analyzed for the expression of HIF-1 as an indicator of tumor hypoxia. A representative blot from several tumor lysate repeats with similar outcomes is shown.  $\beta$ -actin was used as a loading control. Densitometric analysis of all the western blots were quantified by ImageJ software and the mean densitometry values were plotted in terms of relative protein expression. **(B)** HIF-1 proteins were depleted in RAW macrophages by siRNA-based methods and the macrophages were then irradiated with a dose of 2 Gy and the impact of this treatment was

analyzed on the level of NO in the cell culture supernatants. **(C)** RAW macrophages treated with various doses of CoCl<sub>2</sub> (to stabilize the expression of HIF-1) were stimulated with Th1 effectors (i.e. LPS and IFN $\gamma$ ) and NO levels were quantified 24h post treatment by using a Giess reagent method. **(D)** Naive RAW macrophages were treated with CoCl<sub>2</sub> and the impact of treatment on the levels of NO were analyzed. Shown is the mean level ( $\mu$ M) of NO  $\pm$  SEM from three independent experiments. **(E)** Expression of iNOS in CD11b+/Gr-1(-) RT5 tumor macrophages under the influence of CoCl<sub>2</sub> treatment was analyzed. Statistical analyses were conducted using either Student's t tests, 1 way or 2 way ANOVA, followed by Bonferroni post-test (\*P < 0.05; \*\*P < 0.01; \*\*\*P < 0.001). All the statistical analyses was carried out with GraphPad Prism Version 7.0 software.

**A**



**B**

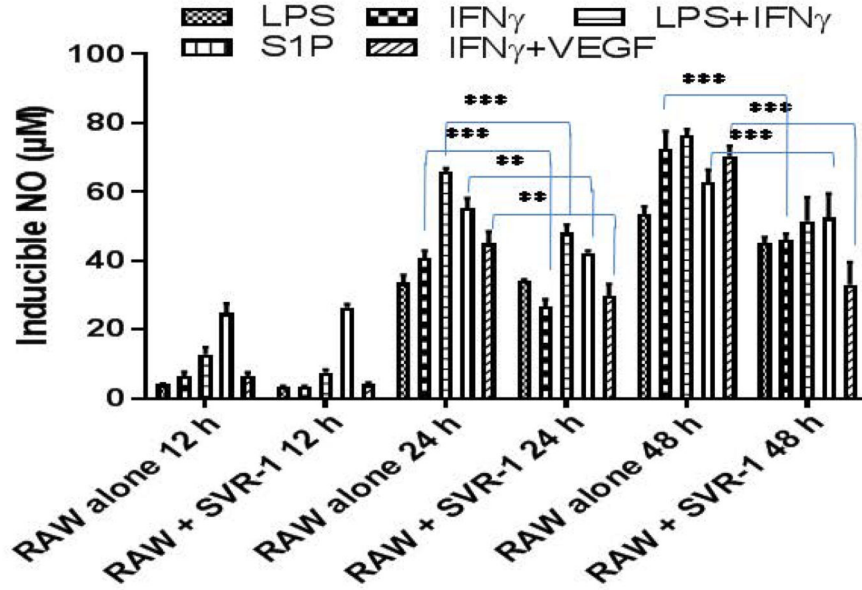
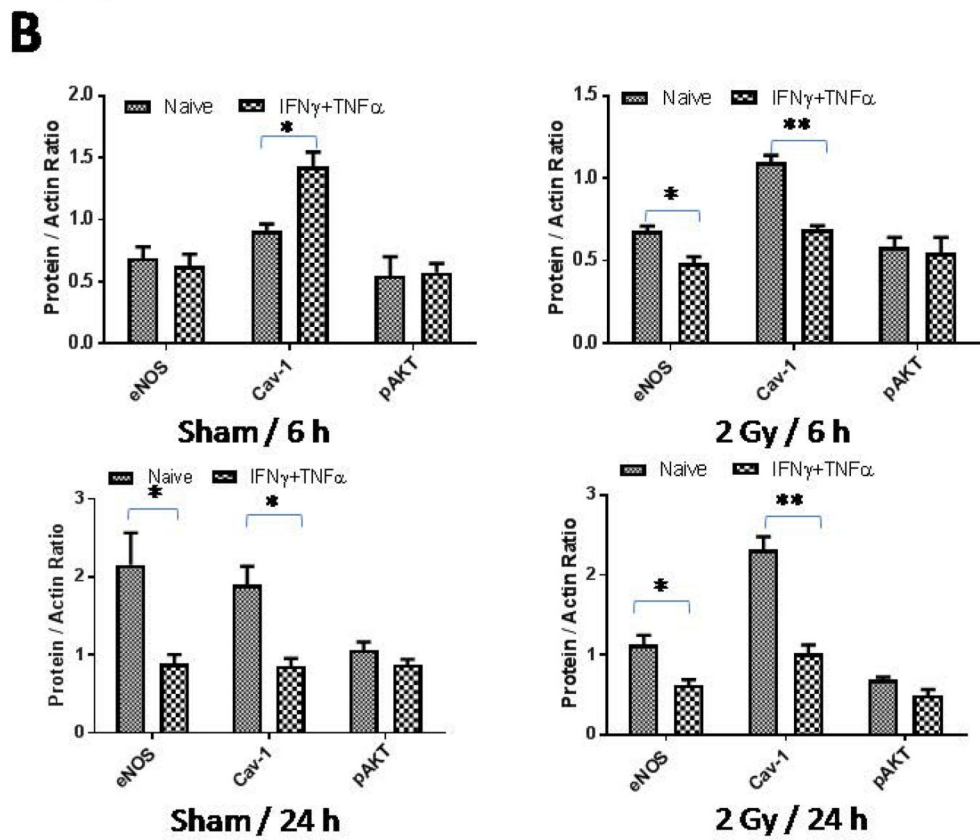
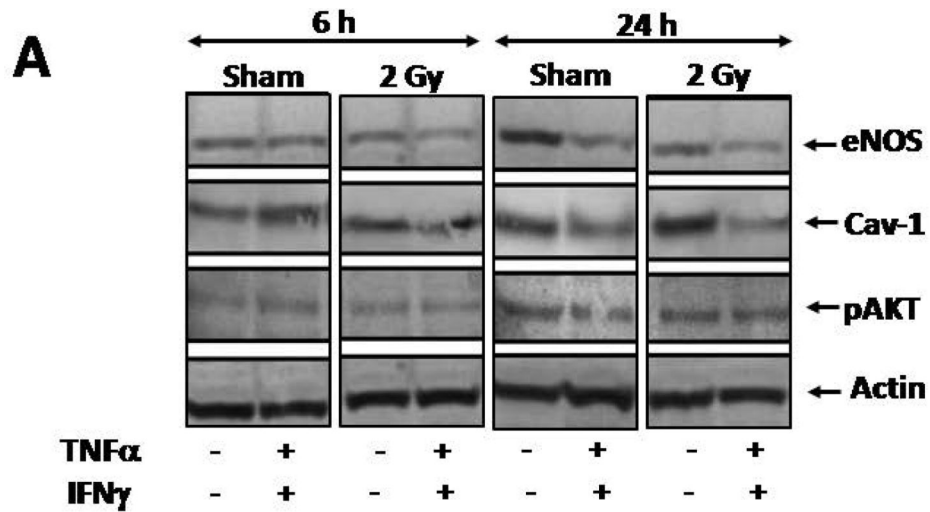


**Figure 2. VEGFR2+ tumor-derived endothelium inhibits M1programming of naive macrophages.**

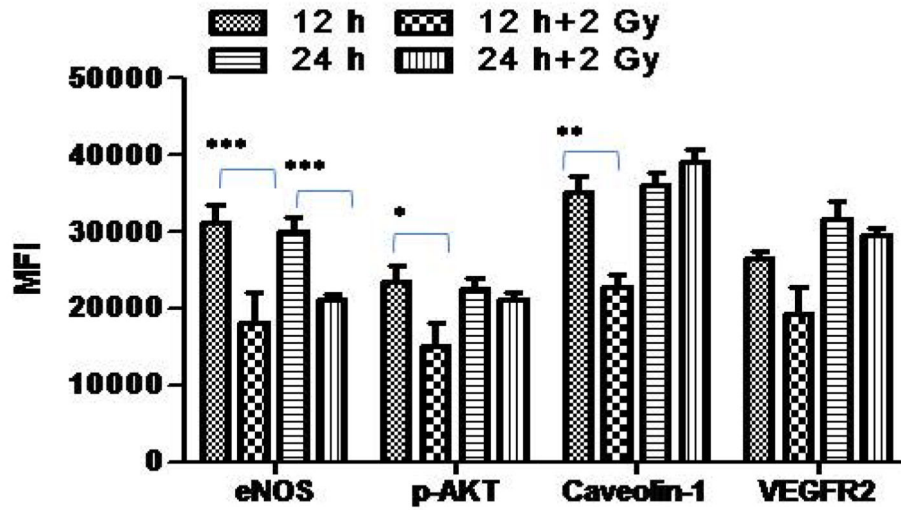
(A) Naive RAW macrophages were cultured with or without SVR endothelium and NO was quantified in the culture supernatant at the indicated time intervals. (B) RAW macrophages were cultured with SVR cells and were stimulated as indicated and NO levels were quantified in the culture supernatant at the indicated time intervals. Shown are the mean levels of NO ( $\mu\text{M}$ ) $\pm$ SEM from three independent experiments. Statistical analysis was

conducted using a two-tailed paired t-test with 95% confidence intervals (\* $p < 0.05$ ; \*\* $p < 0.01$ ).





**C**



**D**

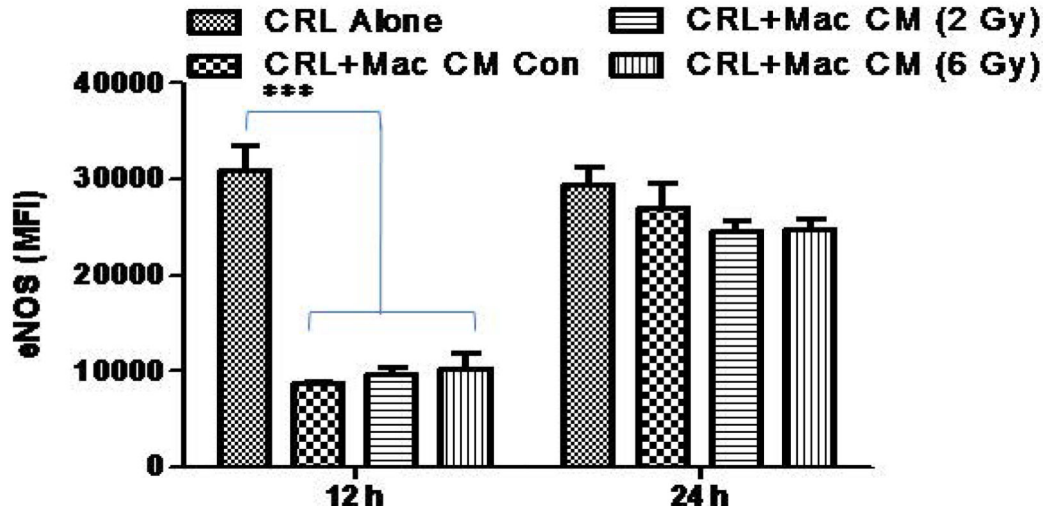


**Figure 3. Gamma irradiation modifies impermeable VEGFR2+ tumor-derived endothelium.** (A) VEGFR2+ pancreatic  $\beta$ -islet SVR (derivative of SVEN) endothelial cells were irradiated with gamma irradiation (2Gy) viz-a-viz stimulation with Th1 effector cytokines and the impact of their stimulation was analyzed on the expression of key proteins involved in eNOS signaling/angiogenesis at 6 h and 24 h post treatment/irradiation. Shown is a representative western blot from 3 independent experiments.  $\beta$ -actin was used as a loading control. (B) Densitometry quantification of representative western blots shown under A were analyzed by Image J and the data were plotted as a mean of protein/actin ratio. Statistical

analysis was conducted using a two-tailed paired t-test with 95% confidence intervals (\* $p < 0.05$ ; \*\* $p < 0.01$ ). **(C)** SVR cells cultures were irradiated (2 Gy) and eNOS proteins were quantified using a fluometric-based method at the indicated time intervals. Similarly, **(D)** SVR cells were cultured in the presence of conditioned media obtained from naïve or irradiated mouse peritoneal macrophages and levels of eNOS proteins were quantified using a fluometric-based method at the indicated time intervals

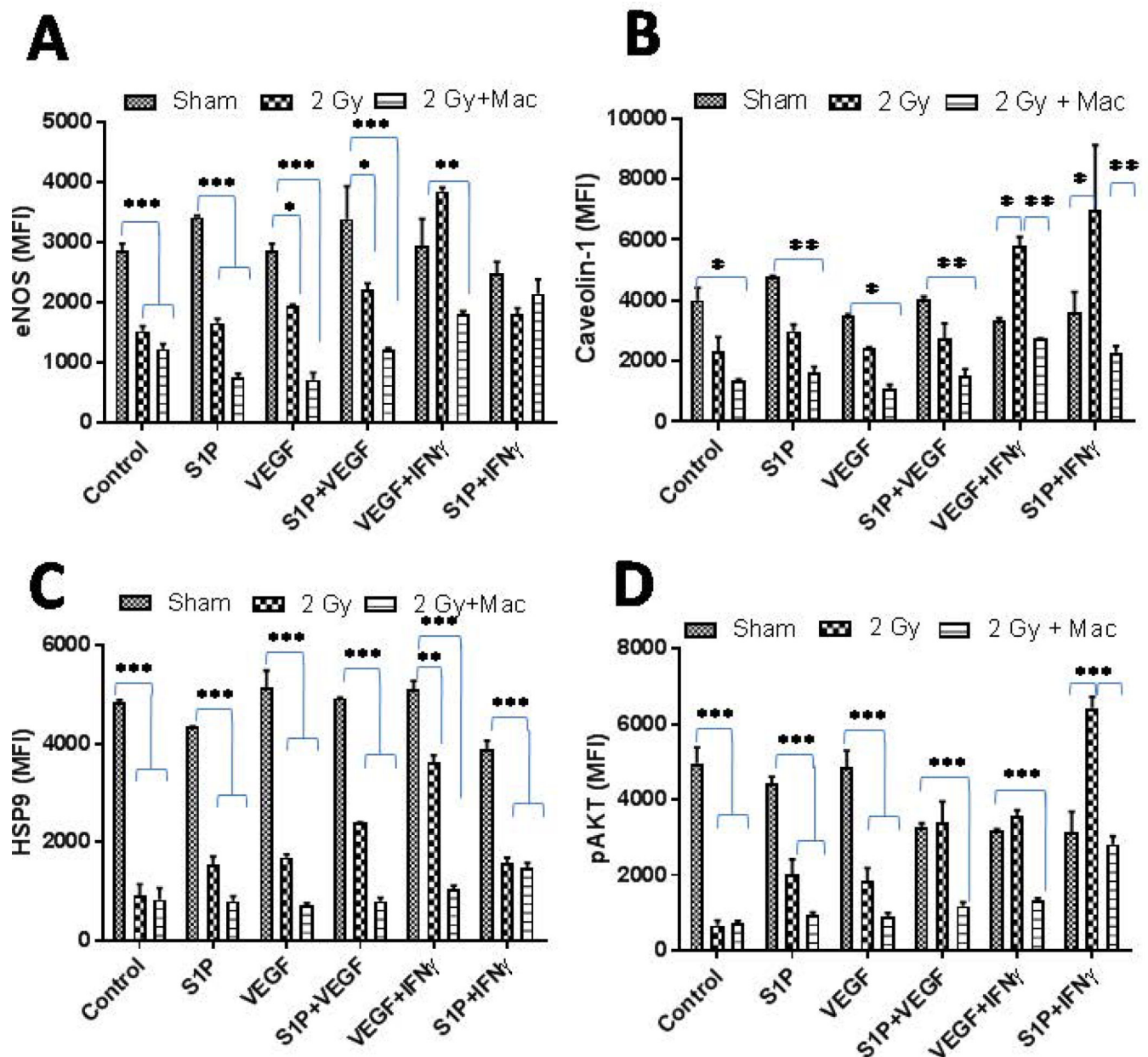


**Figure 4. Gamma radiation inhibits angiogenic responses in primary endothelium.**

Freshly isolated HUVEC endothelial cells were irradiated upon treatment with or without conditioned media obtained from M1-differentiated macrophages and the impact of these treatments was analyzed on various proteins involved in angiogenic signaling. Shown are the MFI of proteins  $\pm$  SEM from three independent experiments. Statistical analyses were conducted using either Student's t tests or 2 way ANOVA followed by Bonferroni post-test (\* $P < 0.05$ ; \*\* $P < 0.01$ ; \*\*\* $P < 0.001$ ).